Reversible insulin resistance in muscle and fat unrelated to the metabolic syndrome in patients with acromegaly

Mai C. Arlien-Søborg,[a,b]* Jakob Dal,[a,c,d] Michael Alle Madsen,[a,e] Morten Lyng Høgild,[a,b] Astrid Johannesson Hjelholt,[a,b] Steen B. Pedersen,[f] Niels Møller,[a,b] Niels Jessen,[f,g,h] and Jens O.L. Jørgensen,[a,b]

[a]Department of Endocrinology and Internal Medicine, Aarhus University Hospital, Denmark
[b]Medical Research Laboratory, Department of Clinical Medicine, Aarhus University Hospital, Denmark
[c]Department of Endocrinology, Aalborg University Hospital, Denmark
[d]Steno Diabetes Centre North, Aalborg University Hospital, Aalborg, Denmark
[e]Department of Nuclear Medicine & PET Centre, Aarhus University Hospital, Denmark
[f]Steno Diabetes Centre, Aarhus, Denmark
[g]Department of Clinical Pharmacology, University of Aarhus, Aarhus, Denmark
[h]Department of Biomedicine, Aarhus University, Denmark

Summary

Background Patients with active acromegaly exhibit insulin resistance despite a lean phenotype whereas controlled disease improves insulin sensitivity and increases fat mass. The mechanisms underlying this paradox remain elusive, but growth hormone (GH)-induced lipolysis plays a central role. The aim of the study was to investigative the molecular mechanisms of insulin resistance dissociated from obesity in patients with acromegaly.

Methods In a prospective study, twenty-one patients with newly diagnosed acromegaly were studied at diagnosis and after disease control obtained by either surgery alone (n=10) or somatostatin analogue (SA) treatment (n=11) with assessment of body composition (DXA scan), whole body and tissue-specific insulin sensitivity and GH and insulin signalling in adipose tissue and skeletal muscle.

Findings Disease control of acromegaly significantly reduced lean body mass ($p<0.001$) and increased fat mass ($p<0.001$). At diagnosis, GH signalling (pSTAT5) was constitutively activated in fat and enhanced expression of GH-regulated genes (CISH and IGF-I) were detected in muscle and fat. Insulin sensitivity in skeletal muscle, liver and adipose tissue increased after disease control regardless of treatment modality. This was associated with enhanced insulin signalling in both muscle and fat including downregulation of phosphatase and tensin homolog (PTEN) together with reduced signalling of GH and lipolytic activators in fat.

Interpretation In conclusion, the study support that uncontrolled lipolysis is a major feature of insulin resistance in active acromegaly, and is characterized by upregulation of PTEN and suppression of insulin signalling in both muscle and fat.

Funding This work was supported by a grant from the Independent Research Fund, Denmark (7016-00303A) and from the Alfred Benzon Foundation, Denmark.

Keywords: Growth hormone; Acromegaly; Lipolysis; Insulin resistance; Insulin signalling

EBioMedicine 2022;75: 103763
Published online xxx
https://doi.org/10.1016/j.ebiom.2021.103763

Introduction

Acromegaly caused by sustained growth hormone (GH) hypersecretion from a benign pituitary adenoma is of insidious onset and most patients develop complications several years prior to diagnosis.[1]

Growth hormone excess induces insulin resistance in skeletal muscle and liver, which may progress to overt diabetes mellitus[2,3] and is causally linked to GH-induced lipolysis.[4] The underlying molecular mechanisms remain unclear, but substrate competition between glucose and fatty acids,[5,6] reduced muscle

*Corresponding author at: Department of Endocrinology and Internal Medicine, Aarhus University Hospital, Denmark.
E-mail address: mas@clin.au.dk (M.C. Arlien-S½borg).

Research in context

Evidence before this study

Insulin resistance and a lean phenotype coexist in patients with active acromegaly. Disease control of acromegaly normalizes insulin sensitivity despite a concomitant increase in fat mass and decrease in lean body mass. Experimental studies in human subjects demonstrate that growth hormone (GH) - induced insulin resistance is causally linked to activated lipolysis

Added value of this study

Uncontrolled lipolysis is a major feature of insulin resistance in acromegaly, which is accompanied by upregulation of PTEN and suppression of insulin signalling in both muscle and fat

Implications of all the available evidence

Acromegaly constitutes a unique disease model to understand fatty acid-driven insulin resistance unrelated to the metabolic syndrome and may identify novel treatment targets

glycogen synthase activity[2,7] and impaired insulin signalling[8] are reported.

Insulin resistance is generally associated with obesity and reduced lean body mass (LBM) as part of the metabolic syndrome, and may be reversed by life style interventions that promote fat loss and increase physical activity and LBM.[9] Paradoxically, patients with active acromegaly are insulin resistant despite a lean phenotype, and disease control restores insulin sensitivity in concomitance with increased fat mass and reduced LBM.[10–12]

Somatostatin analogue (SA) treatment acts on the pituitary gland to suppress GH hypersecretion and tumour growth.[13] In addition, somatostatin suppresses insulin secretion and thereby impairs glucose tolerance and promotes lipolysis,[14–16] but it also stimulates muscle glucose uptake and inhibits glucagon secretion.[16–18] A GH receptor antagonist is also available and can be used in combination with SA.[19–21]

Acromegaly constitutes a unique human *in vivo* model to study reversible insulin resistance and our study aim was to use this model to investigative the molecular mechanisms of insulin resistance dissociated from obesity. We studied twenty-one patients with newly diagnosed acromegaly before and after disease control obtained by either surgery or medical treatment. The investigations included assessment of body composition, glucose tolerance, basal and insulin stimulated substrate metabolism, and *in vivo* GH and insulin signalling in adipose tissue and skeletal muscle.

Methods

Patients

In a prospective study, twenty-one newly diagnosed patients with acromegaly were recruited from 2007 to 2016, and studied shortly after confirmation of the diagnosis (pre) and after disease control (post). Ten patients were controlled by trans sphenoidal surgery only (Surgery), whereas eleven patients, of whom six had undergone prior surgery, required SA treatment (SA). Three of the SA patients were co-treated with pegvisomant; unless otherwise specified, these three patients are included in the SA group. The study population is considered to be representative of the acromegaly patient population.[1] Disease activity was assessed by age- and gender adjusted insulin-like growth factor I (IGF-I) levels and GH levels obtained during an oral glucose tolerance test (OGTT). The OGTT was performed by measuring serum glucose 60 minutes prior to and 150 minutes after a 75 g oral glucose load.

For the metabolic studies, each patient was studied on a separate occasion for six hours after an overnight fast including a 4h basal period followed by a 2h hyperinsulinemic, euglycemic glucose clamp (HEC). An intravenous glucose tracer was concomitantly administered. Blood samples were drawn in triplicates at the end of the basal period and the HEC. Indirect calorimetry and muscle and fat biopsies were obtained in the basal period and during the HEC at t=60 min and t=270 min, respectively. Body composition was assessed by dual x-ray absorptiometry (DXA).

Hormones and metabolites

Serum GH and IGF-I levels were measured using chemiluminescence technology (IDS-iSYS platform; Immunodiagnostic 141 Systems, Boldon, UK). Serum IGF-I values were also expressed as standard deviation scores (IGF-SDS) based on age- and gender-specific IGF-I reference values.[22] During the HEC, point of care plasma glucose was measured using an YSI 142 2300 STAT Plus glucose analyser (YSI, Burlington, VT). Additional serum samples were stored at -20°C and assayed in the same run after study completion. Insulin was analysed by commercial ELISA (Dako, Glostrup, Denmark), as was C-peptide (ALPCO, Salem, NH, USA) and free fatty acids (FFA) (Wako Chemicals, Neuss, Germany). Plasma glucagon concentrations were determined by a radioimmunoassay (EMD Millipore, Darmstadt, Germany).

Glucose metabolism and insulin sensitivity

A constant insulin infusion of 1 mU/kg total body weight (TBW)/min (Actrapid, Novo Nordisk, Denmark) was administered during the HEC, and the plasma glucose level was clamped at ≈ 5 mmol/l by adjusting the rate of an intravenous 20% glucose infusion based on

glucose measurements every 10 minute. The M value was calculated as the mean glucose infusion rate (GIR) per kg TBW at steady state. To quantify glucose turnover, a primed continuous infusion of [3-3H]-glucose was administered during the 6-h study period (bolus 20 µCi followed by 0.12 µCi/min; NEN Life Science Products, Boston, MA, USA). The specific activity of [3-3H] glucose was measured at 10-min intervals in the basal state and in the HEC and Steele's non-steady-state equation was applied to calculate the glucose rate of appearance (Ra) and rate of disappearance (Rd). Endogenous glucose production (EGP) during the HEC was calculated by subtracting mean GIR from Ra. Non-oxidative glucose disposal (NOGD) was determined by subtracting oxidative glucose disposal from total glucose disposal (Rd). The area under the glucose curve (AUC) during the OGTT was calculated using the trapezoidal rule. Homeostatic model assessment (HOMA) was used to calculate β-cell function (HOMA-β) and insulin resistance (HOMA-IR) based on fasting levels of glucose and insulin using standard equations.[23] The adipose tissue insulin resistance index (Adipo-IR index) was calculated by multiplying basal state serum insulin concentration (pmol/l) with serum FFA concentration (mmol/l), which correlates well with the gold standard measure for insulin sensitivity in adipose tissue.[24]

Arterio-venous substrate balances

A catheter was placed retrograde in a deep antecubital vein and a second catheter was inserted in a heated dorsal vein on the contralateral arm to sample arterialized blood. Total forearm blood flow was determined by venous occlusion plethysmography.[25] Substrate balances across the forearm were calculated by multiplying the arteriovenous differences and the blood flow.

Body composition

Body composition was measured by DXA (QDR-2000; Hologic, Marlborough, MA, USA) and total body fat (TBF %) and truncal fat (neck, trunk and pelvis) were computed according to the manufacturer's software.

Indirect calorimetry

Resting energy expenditure (REE) was determined by indirect calorimetry (Oxycon Pro; Intramedic, Gentofte, Denmark) during a 15-min collection period and adjusted for LBM.[26] Glucose oxidation rates were calculated after correction for protein oxidation based on urinary urea excretion.[27]

Muscle biopsies

During sterile conditions and local anaesthesia, muscle biopsies were obtained from the vastus lateralis of the quadriceps femoris muscle 10-15 cm proximal of the patella using a Bergström biopsy needle. The muscle tissue was immediately snap-frozen in liquid nitrogen and stored at −80°C until use.

Adipose tissue biopsies

Adipose tissue biopsies were obtained by liposuction from the abdominal subcutaneous fat depots lateral to the umbilicus during local anaesthesia. The tissue was immediately washed free of blood, snap-frozen in liquid nitrogen and stored at −80°C until use.

Western blotting

Frozen muscle biopsies were freeze-dried prior to homogenization in Precellys 24 homogenizer (Bertin Technologies, France) using a cold buffer containing a protease inhibitor cocktail (Halt, Thermo Scientific, USA), 20 mM Tris, 50 mM NaCl, 50 mM NaF, 5 mM Na4P2O7, 5 mM NAM, 5 μM TSA, 250 mM sucrose, 1% (v/v) Triton X-100 and 2 mM DTT, pH7.4. Samples were rotated for 20 minutes at 4°C and centrifuged at 14.000 g for 20 minutes at 4°C. Total protein content was determined by the Bradford protein assay (Bio-Rad). Applying the CriterionXT-system (Bio-Rad), western blots were performed on StainFree 4−15% sodium dodecyl sulphate polyacrylamide gel electrophoresis gels and proteins transferred onto polyvinylidene difluoride (PVDF) membranes blocked for 2 h in 0.3% iBlock. The PVDF membranes were incubated with primary antibodies (AB) overnight and re-incubated for 1 h with horseradish peroxidase -conjugated secondary AB to visualize proteins by enhanced chemiluminescence using a ChemiDoc XRS system (Bio-Rad). Protein signals were quantified using Image Lab (version 4.0.1, Bio-Rad). The Bio-Rad Stain Free technique was used as a loading control as validated previously.[28] Protein phosphorylation is expressed as a ratio to total protein level. Detailed information regarding the antibodies is provided in the supplementary material table 1.

Capillary electrophoresis immunoassay (WES)

Adipose tissue (AT) biopsies were analysed by a capillary electrophoresis immunoassay (Wes; ProteinSimple, Santa Clara, CA, USA) as previously described.[29] The tissue was homogenized using a tissue lyser (Precellys 24: Bertin technologies, France) in a buffer containing 50 mM HEPES, 137 mM NaCl, 10 mM Na4P2O7, 20 mM NaF, 5 mM EDTA, 1 mM $MgCl_2$, 1 mM $CaCl_2$, NP-40, 2 mM NaOV, 5 mM NAM, 10 μM TSA, NP-40, HALT, glycerol and demineralized water. The samples were spun at 1300 RPM for 20 min after 1 hour of agitation at 40°C with only the infranatant used for analyses. Bicinchoninic acid assays measured protein concentration and the expression was quantified as peak area for the protein of interest. Protein phosphorylation is expressed as a ratio to total protein level. Detailed

information regarding the antibodies is provided in the supplementary material table 1.

Real-time qRT-PCR

RNA was extracted from the biopsies using TRIzol (Gibco BRL, Life Technologies, Roskilde, Denmark). The amount and purity of total RNA were quantified using a NanoDrop 8000 Spectrophotometer (Thermo Scientific Pierce, Waltham, Maine, USA). Integrity of the RNA was checked by visual inspection of the two ribosomal RNAs on an agarose gel. cDNA was synthesized using Verso cDNA kit (cat# Ab-1453, Thermo Fischer Scientific) with random hexamer primers. PCR were performed in duplicate using LightCycler SYBR Green master mix (Roche Applied Science) in a LightCycler 480 (Roche Applied Science) and the increase in fluorescence was measured in real time during the extension step. B2M (encoding β2 microglobulin) was used as housekeeping gene, as mRNA levels were similar between interventions and groups. Detailed information regarding primer and probe sequences is provided in the supplementary material table 2.

Role of Funders

The study funder was not involved in the design of the study; the collection, analysis, and interpretation of data; writing the report; and did not impose any restrictions regarding the publication of the report.

Statistics

Results are presented as mean ± SEM when normally distributed or otherwise as median (CI). Baseline comparisons were done by unpaired Student t test if the data were normally distributed, and the Mann-Whitney rank sum test was used for non-normally distributed data. Normality was checked by QQ-plots, and equal variance was assessed by Levene's test. If skewed, the data were logarithmically transformed. Effects of intervention were tested by a two-way repeated measurement mixed model analysis. The model included intervention (active (pre) vs. controlled disease (post)), group (Surgery vs. SA) and sample time (basal vs. HEC). Post hoc comparisons were conducted in case of a significant interaction. Only significant effects of treatment modality are stated in the results section. Sub analysis was performed within the medically treated group where considered pertinent. Normality of the residuals was checked by histogram and QQ plot and if skewed, appropriate logarithmic transformation was used before statistical testing. Kenward Roger's approximation was used for calculation of degrees of freedom to account for unbalanced data sets because of missing observations. Correlation analysis was performed with Pearson's or Spearman's coefficient for normally and non-normally distributed variables, respectively. P values <0.05 were considered significant. The sample size was defined based on a previous study.[10] The primary outcome was insulin sensitivity, expressed as the *M* value. To detect a clinically significant change in the *M* value of 2.5 mg/kg/min, a sample size of 9 was required using α=0.05 and β=0.9, To ensure reasonable power for evaluation of treatment modality as well as secondary endpoints, twenty-one patients were included in the study. Secondary outcomes were hepatic and adipose tissue insulin sensitivity as well as GH and insulin signalling in adipose tissue and skeletal muscle. Statistical analyses were performed with Stata Statistical Software, release 15 (StataCorp LP, College Station, TX, USA). The graphical presentations were made in SigmaPlot 11.0 (Systat Software, San Jose, CA, USA).

Ethics

The study was approved by the Central Denmark Region Scientific Ethics Committee (M-20070130), registered at ClinicalTrials.gov (NCT00647179) and conducted in agreement with the Declaration of Helsinki II. Written informed consent was obtained from all subjects before inclusion in the study.

Results

Patient characteristics

The majority of patients harboured a pituitary macro adenoma (19/21) with mean IGF-I_{SDS} levels of 4.5 ± 0.4 and mean GH_{nadir} levels of 5.55 (0.38; 29.3) µg/l. At the time of diagnosis, the patients controlled by surgery only and those controlled by SA were comparable regarding age, sex, adenoma size and disease activity (Table 1). The time elapsed between first and second visit was 44 (16; 163) weeks and IGF-I_{SDS} and GH_{nadir} (excluding the three pegvisomant treated patients) declined to 1.2 ± 0.3 and 0.46 (0.28; 0.74) µg/l, respectively (Table 1). Four male patients presented with mild biochemical hypogonadism, which remained unreplaced during the study period; one of these 4 patients also presented with mild hyperprolactinemia which resolved after disease control without altering the serum testosterone level. Two patients received metformin treatment for type 2 diabetes, which was discontinued after disease control in one of the patients.

Body composition

The median weight (kg) remained unchanged after disease control (p= 0.642) whereas disease control significantly increased TBF % [23.0 (19.3; 26.6) (pre) vs. 27.8 (24.2; 31.5)) (post), p< 0.001] and in particular truncal fat (kg) [9.4 (7.5; 11.3) (pre) vs. 12.3 (10.4; 14.2) (post), p< 0.001]. Nine patients (5 females and 4 males) were obese after disease control as defined by a TBF % of > 30% (females) and 25 % (males), respectively,[30] of

	SA (n=11)	Surgery (n=10)	*P-value*
Sex (M/F)	5/6	5/5	0.83
Age (years)			
Pre	52 ± 3.8	50 ± 4.9	0.72
Post	53 ± 3.9	51 ± 4.7	0.73
BMI			
Pre	28.7 ± 1.6	26.9 ± 1.1	0.40
Post	28.6 ± 1.6	26.3 ± 1.4	0.30
Adenoma size			0.94
Macro	10	9	
Micro	1	1	
GH, nadir (µg/l)			
Pre	6.3 (2.4; 16.3)	4.9 (2.2; 10.7)	0.66
Post	0.6 (0.2; 1.6)*	0.4 (0.2; 0.7)	0.19
IGF-I (µg/l)			
Pre	739 ± 85	649 ±76	0.44
Post	214 ± 35	209 ± 25	0.91
IGF-I_{SDS}			
Pre	4.7 ± 0.3	4.3 ± 0.5	0.46
Post	1.1 ± 0.5	1.2 ± 0.4	0.99
Fasting glucose (mmol/L)			
Pre	5.6 (5.1; 6.1)	5.9 (5.3; 6.5)	0.48
Post	5.7 (5.3; 6.3)	4.9 (4.4; 5.4)	0.03
HbA1c (mmol/mol)			
Pre	40 (35; 45)	43 (38; 49)	0.45
Post	41 (35; 46)	36 (30; 41)	0.23
Time btw. study days (weeks)	58 (16; 163)	29 (18; 47)	0.05
Surgery (y/n)	6/5	10/0	0.01
Radiation therapy (y/n)	0/11	0/10	NA
Dopamine agonist (y/n)	1/10	1/9	0.94
Diabetes mellitus (y/n)	0/11	1/9	0.28
Anterior pituitary deficiency (y/n)	3/8	1/9	0.70

***Table 1*: Patient characteristics**
*Exclusion of patients treated with a GH-antagonist
Patient characteristics at time of diagnosis and after disease control according to treatment modality; Somatostatin analogue (SA) and Surgery. Data are presented as total number, mean ± SEM or median (CI) when logarithmically transformed. Time since intervention is presented as mean and range. The two groups were comparable at all listed variables.

which two females and two males were obese before disease control. Median LBM (kg) decreased after disease control irrespective of disease modality [64.9 (58.5; 71.2) (pre) vs. 60.7 (54.3; 67.1) (post), p< 0.001] (Table 2). The change in TBF correlated negatively with the corresponding change in IGF-I (r= -0.67, p= 0.001) whereas the change in LBM correlated positively with both ΔIGF and ΔGH (excluding pegvisomant

	Pre	Post
Weight (kg)	89.1 (81.3; 96.9)	88.5 (80.7; 96.4)
Total fat mass (kg)	20.0 (16.2; 23.9)	24.4 (20.6; 28.3)[a]
Total body fat (%)	23.0 (19.3; 26.6)	27.8 (24.2; 31.5)[a]
Trunk fat mass (kg)	9.4 (7.5; 11.3)	12.3 (10.4; 14.2)[a]
Lean body mass (kg)	64.9 (58.5; 71.2)	60.7 (54.3; 67.1)[a]
Resting energy expenditure (kcal/24 h)	1901 (1818; 1984)	1726 (1643; 1810)[a]

***Table 2*: Body composition**
Body composition and resting energy expenditure before (pre) and after (post) disease control in the entire cohort measured by dual-energy X-ray absorptiometry. Data are presented as median (CI).
[a] $P < 0.05$ for pre total vs post total.

treated patients) [r= 0.60, p= 0.0043 (IGF-I); r= 0.68, p= 0.0029 (GH)].

Resting energy expenditure and glucose oxidation rates

Median REE (kcal/24 h) significantly decreased after disease control [1900 (1817; 1983) (pre) vs. 1726 (1642; 1809) (post), p< 0.001] (Table 2). ΔIGF-I correlated positively with Δ REE in the basal state (r = 0.56, p= 0.0236).

Circulating hormones and metabolites

Disease control induced a significant decrease in basal median insulin levels (pmol/L) [71.1 (56.5; 89.6) (pre) vs. 28.6 (22.7; 36.0) (post), <0.001] most markedly in the SA group [-64.1 (-100.1; -28.1) (Δ SA) vs -23.2 (-81.4; 35.1) (Δ Surgery), p= 0.042] (Table 3). Disease control also decreased the median glucagon levels (pg/mL) during the HEC [51.0 (42.8; 59.2) (pre) vs. 44.4 (36.2; 52.6) (post), p= 0.004], which again was more pronounced in the SA group [-6.63 (-12.6; -0.64) (Δ SA) vs 2.42 (-3.24; 8.08) (Δ Surgery), p=0.029]. Median glucose levels (mmol/L) decreased insignificantly in the basal state after disease control [5.7 (5.3; 6.1) (pre) vs. 5.4 (5.0; 5.7) (post), p= 0.14], but treatment modality impacted differentially such that an increase was observed in the SA group as opposed to a decrease in the Surgery group [0.17 (-0.11; 0.45) (Δ SA) vs -1.23 (-3.10; 0.51) (Δ Surgery), p=0.011] (Table 3). The basal median FFA levels were similar before and after disease control, whereas the insulin-stimulated reduction in FFA levels during the HEC was more pronounced after disease control (p < 0.001), irrespective of treatment modality (Fig. 1).

Glucose tolerance, insulin sensitivity and glucose turnover

Mean serum glucose levels during the OGTT before and after disease control are shown in Fig. 2. Glucose tolerance, expressed as area under the glucose curve (AUC_{0-210} mmol/L·min), was unaltered after disease control in the whole group [1628.2 (1467.3; 1806.8) (pre) vs. 1553.0 (1396.9; 1726.4) (post), p= 0.373]. However, SA treatment expectedly induced glucose intolerance compared to Surgery (Fig. 2 and Table 4), and the 2h glucose value was significantly higher in the SA treated group [1.138 (-0.090; 2.365) (Δ SA) vs. -1.64 (-3.96; 0.68) (Δ Surgery), p=0.037]. Disease control reduced basal insulin resistance (HOMA-IR) and beta cell function (HOMA- β) and the latter more so after SA treatment (Table 3). Disease control improved insulin sensitivity during the HEC (mg/kg/min) by more than 40% [3.34 (2.50; 4.19) (pre) vs. 4.80 (3.98; 5.63) (post), p= 0.001], regardless of treatment modality (p= 0.58) (Fig. 3) and adjustment for the use of metformin did not alter the results. In an exploratory secondary sub analysis, insulin sensitivity during the HEC increased

	Pre	Post	Δ SA	Δ Surgery
Glucose (mmol/l)				
Basal	5.71 (5.33; 6.11)	5.36 (5.0; 5.74)	0.17 (-0.11; 0.45)	-1.23 (-3.10; 0.51)[b]
HEC	5.15 (4.81; 5.51)	5.02 (4.69; 5.38)	0.12 (-0.16; 0.39)	-0.05 (-1.49; 0.47)
Insulin (pmol/L)				
Basal	71.1 (56.5; 89.6)	28.6 (22.7; 36.0)[a]	-64.1 (-100.1; -28.1)	-23.2 (-81.4; 35.1) [b]
HEC	338.7 (268.8; 426.8)	351.4 (278.9; 442.8)	6.13 (-40.2; 52.4)	11.7 (-46.6; 70.0)
HOMA-IR (mmol/L * pmol/L)				
Basal	3.01 (2.17; 4.17)	1.13 (.82; 1.57)[a]	-2.56 (-4.08; -1.04)	-1.68 (-4.29; 0.92)
HOMA-β (pmol/L / mmol/L)				
Basal	113.9 (78.2; 166.0)	54.1 (37.2; 78.9)[a]	-113.1 (-174.0 -52.2)	23.1 (-152.1; 198.2)
C-peptide (pmol/L)				
Basal	626.2 (468.4; 784.0)	364.3 (203.6; 525.0)[a]	-184.7 (-395.8; 26.5)	-374.2 (-703.4; -45.0)
HEC	420.8 (261.6; 580.0)	268.4 (107.7; 429.1)[a]	-195.3 (-346.7; -44.0)	-179.3 (-411.2;52.7)
Glucagon (pg/mL)				
Basal	55.0 (46.8; 63.2)	52.4 (44.2; 60.6)	-6.63 (-12.6 -0.64)	2.42 (-3.24; 8.08) [b]
HEC	51.0 (42.8; 59.2)	44.4 (36.2; 52.6)[a]	-10.4 (-14.6; -6.16)	-1.89 (-9.81; 6.02)[b]
Free Fatty Acids (mmol/L)				
Basal	0.39 (0.30; 0.51)	0.41 (0.32; 0.53)	0.00 (-0.12; 0.13)	0.01 (-0.13; 0.15)
HEC	0.07 (0.05; 0.09)	0.04 (0.03; 0.05)[a]	-0.06 (-0.11; -0.00)	-0.03 (-0.05; 0.00)

***Table 3*: Circulating hormones**

Circulating hormones before (pre) and after (post) disease control in the entire cohort, and according to treatment modality (Somatostatin Analogue (SA) and Surgery) presented as change (Δ) from first to second visit. HEC = hyperinsulinemic, euglycemic glucose clamp. All data are presented as median (CI).

[a] $P < 0.05$ for pre total vs post total.

[b] $P < 0.05$ for Δ pre-post, SA vs. surgery.

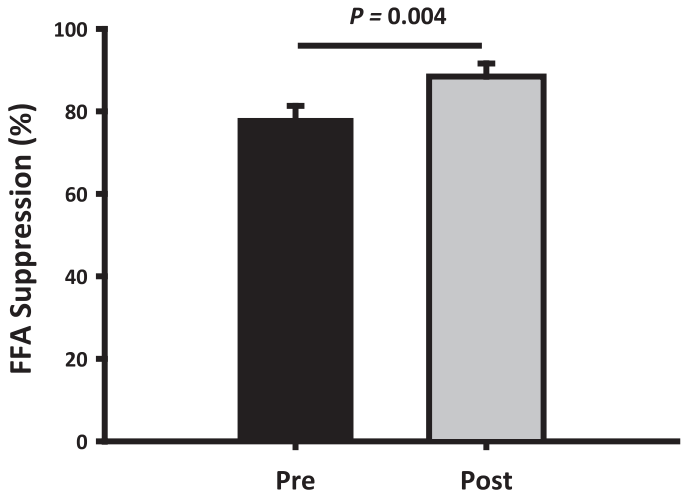

Fig. 1. Free fatty acids

Mean ± SEM reduction (%) in serum free fatty acids (FFA) from the basal period to the HEC before (pre) and after (post) disease control**.** Suppression of FFA levels was more pronounced after disease control (p = 0.004)

to a similar in the following treatment groups: Surgery only, SA with prior surgery, and SA without prior surgery (data not shown). The overall reduction in insulin sensitivity was paralleled by increased isotopically measured glucose disposal (mg/kg/min) during the HEC [4.28 (3.60; 4.96) (pre) vs. 5.37 (4.74; 6.00) (post), p= 0.009], irrespective of treatment modality (p= 0.118) and accompanied by a reduction in both basal and insulin stimulated EGP (Fig. 3). The rate of basal NOGD (mg/kg/min) increased in the SA group as opposed to a decrease in the Surgery group [0.61 (-0.99; 2.20) (Δ SA) vs. -0.43 (-1.29; 0.43) (Δ Surgery), p= 0.029]. During the HEC, disease control increased the rate of NOGD [1.94 (1.27; 2.61) (pre) vs. 3.09 (2.47; 3.71) (post), p= 0.014] independent of treatment modality (p=0.887). Blood flow was unaltered after treatment in both conditions (data not shown). Forearm glucose uptake (FGU) during the HEC increased after treatment (p= 0.003) and most markedly in the SA group (p= 0.006) (Table 4). Δ GH levels correlated inversely with Δ insulin sensitivity expressed as the M value (r = -0.59, p = 0.0257). Disease control significantly increased adipose tissue insulin sensitivity as determined by the Adipo-IR index (Fig. 3).

GH signalling in muscle and fat

GH receptor signal transduction to Signal transducer and activator of transcription 5 (STAT5) phosphorylation decreased significantly in adipose tissue after disease control (p= 0.023), but was not significantly altered in muscle tissue (Fig. 4). Disease control markedly decreased *IGF-I* mRNA levels in both muscle (p= 0.002) and adipose tissue (p= 0.004). The mRNA levels of *cytokine-inducible SH2-containing protein (CISH)* also declined significantly after disease control in both tissues (Fig. 4). The expression of *Suppressor of cytokine signalling 2 (SOCS2)* mRNA levels decreased after disease control in muscle tissue (p= 0.001) but not in adipose tissue (p=0.407) (Fig. 4).

Insulin signalling in skeletal muscle

Disease control decreased protein expression of phosphatase and tensin homolog (PTEN) (p=0.008) and increased protein kinase B (Akt) serine residue phosphorylation (Akt/pAkt) during the HEC (p= 0.003) (Fig. 5). Insulin-stimulated phosphorylation of Akt substrate of 160 kDa (AS160) tended to increase after disease control in a treatment specific manner implying that an increase mainly occurred in the SA group (data not shown). Insulin-stimulated phosphorylation of glycogen synthase (GS) and glycogen synthase kinase (GSK)α/β and activation of glucose transporter type 4 (GLUT4) did not change overall after disease control, but αGSK and GLUT4 increased in the SA group as opposed to a decrease in the Surgery group during the HEC (data not shown). The change in PTEN protein levels correlated positively with the change in FFA concentrations during the HEC. In addition, the change in PTEN protein levels correlated positively with the change in *IGF-I* mRNA expression in the basal state (r = 0.58, p= 0.0456) and *SOCS2* mRNA expression in the basal state (r = 0.54, p= 0.0570). The mRNA expression of *phosphoinositide-3-kinase regulatory subunit 1 (PIK3r1)*, which is upstream of PTEN and Akt, was downregulated in the basal state after disease control (p=0.018). Phosphorylation of the insulin receptor (pIR) was markedly reduced after disease control, both in the basal state (p= 0.002) and during the HEC (p= 0.025) (Fig. 5), and pIR correlated positively with serum

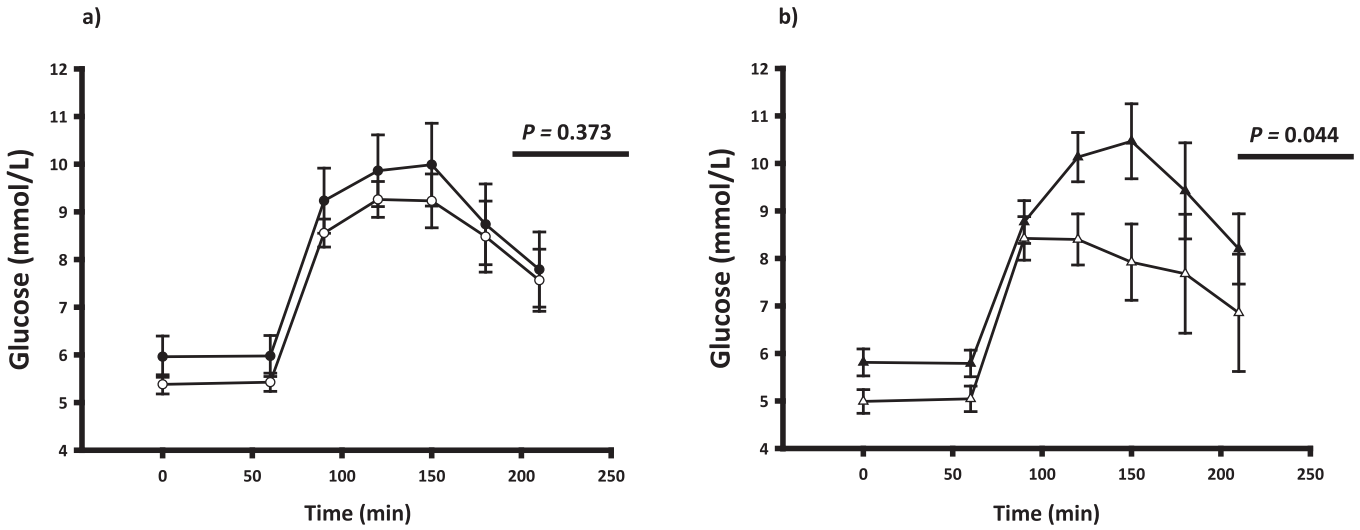

Fig. 2. Glucose tolerance

Plasma glucose levels (mean ± SEM) before and after an oral glucose load (75 g) at t = 60 min. Panel a: All patients not on pegvisomant before (black circle) and after (white circle) disease control. Panel b: After disease control by either surgery only (white triangles) or somatostatin analogue treatment (black triangles). P-values refer to area under the glucose curve (AUC).

	Pre	Post	Δ SA	Δ Surgery
OGTT				
Fasting (mmol/L)	5.76 (5.27; 6.30)	5.32 (4.86; 5.83)	0.41 (-0.19; 1.02)	-1.30 (-2.83; 0.23) [b]
210 min (mmol/L)	7.79 (6.39; 9.19)	7.51 (6.08; 8.93)	1.14 (-0.09; 2.37)	-1.64 (-3.96; 0.68) [b]
Peak (mmol/L)	10.37 (9.29; 11.57)	10.11 (9.05; 11.31)	0.84 (-0.83; 2.51)	-1.31 (-3.80; 1.18)
AUC_{0-210}, (mmol/L·min)	1628 (1467; 1807)	1553 (1397; 1726)	121.5 (-89.9; 332.9)	-290.1 (-750.1;169.9) [b]
Rd_{Glu} (mg/kg/min)				
Basal	2.03 (1.37; 2.69)	1.57 (.94; 2.20)	-0.16 (-0.86; 0.53)	-0.86 (-1.05; -0.36)
HEC	4.28 (3.60; 4.96)	5.37 (4.74; 6.00)[a]	0.61 (-0.13;1.36)	1.77 (1.04; 2.50)
Ra_{Glu} (mg/kg/min)				
Basal	1.95 (1.22; 2.67)	1.43 (.74; 2.12)	-0.33 (.-0.98; 0.33)	-0.67 (-1.01; -0.32)
HEC	3.97 (3.23; 4.72)	4.94 (4.25; 5.63)[a]	0.45 (-0.34; 1.25)	1.87 (0.84; 2.91)
Glucose oxidation (mg/kg/min)				
Basal	1.08 (.82; 1.43)	.95 (.71; 1.26)	0.05 (-1.63; 1.73)	-0.25 (-0.88;0.39)
HEC	1.67 (1.26; 2.22)	1.61(1.21; 2.13)	-0.39 (-1.08; 0.31)	-0.27 (-1.44; 0.91)
Non-oxidative glucose disposal (mg/kg/min)				
Basal	0.59 (-0.08; 1.26)	0.41 (-0.23; 1.06)	0.61 (-0.99; 2.20)	-0.43 (-1.29; 0.43)[b]
HEC	1.94 (1.27; 2.61)	3.09 (2.47; 3.71)[a]	0.82 (-0.78; 2.43)	1.96 (0.48; 3.45)
FGU (μmol/100mL/min)				
Basal	0.19 (0.11; 0.34)	0.18 (0.10; 0.30)	-0.05 (-0.30; 0.19)	-0.09 (-0.30; 0.12)
HEC	0.62 (0.40; 0.98)	1.86 (1.16; 2.97)[a]	1.82 (0.21; 3.43)	0.59 (-1.04; 2.23) [b]

***Table 4*: Glucose metabolism**

*Patients treated with pegvisomant are excluded for evaluation of treatment modality in the analysis of OGTT data.

Glucose metabolism before (pre) and after (post) disease control, and according to treatment modality (Somatostatin Analogue (SA) and Surgery) presented as the change (Δ) from first to second visit. Glucose tolerance was evaluated during an oral glucose (75g) tolerance test. Glucose turnover parameters were determined by [3-^{3}H]-glucose tracer infusion in the basal and HEC periods: $Rd_{Glu,}$ Rate of glucose disappearance; $Ra_{Glu,}$ Rate of glucose appearance. FGU, forearm glucose disposal. Data are presented as median (CI).

[a] $P < 0.05$ for pre total vs post total.

[b] $P < 0.05$ for Δ pre-post, SA vs. surgery.

IGF-I (r =0.68, p= 0.0057) in the basal state before disease control.

The mRNA expression of *angiopoietin-like protein 4 (ANGPTL4)* was reduced after disease control in the insulin stimulated state (p= 0.028).

Insulin signalling and lipolytic regulators in adipose tissue

The protein expression of PTEN decreased significantly after disease control, and this was more pronounced in the Surgery group in the basal state (p=0.014) (Fig. 5). Disease control increased the insulin-stimulated pAkt/Akt ratio (p= 0.007) as well as the mRNA expression of *phosphodiesterase 3b (PDE3b)* (Fig. 5). Protein expression of hexokinase II, which phosphorylates glucose to glucose-6-phosphate, increased in the basal state after disease control (p=0.055), independently of treatment modality (data not shown). Disease control significantly decreased the protein expression of adipose triglyceride lipase (ATGL) as well as the comparative gene identification-58 (CGI58) (Fig. 6). The phosphorylation of hormone sensitive lipase (HSL) also decreased after disease control during the HEC, irrespectively of treatment modality (Fig. 6). The protein and mRNA expression of *fat-specific protein 27 (FSP27)* and the mRNA expression of *G0/G1 switch gene 2 (G0S2)* were unaltered throughout the study period (supplementary material table 3).

Discussion

The present study documents the pronounced and reversible effects of prolonged GH excess on body composition and substrate metabolism in patients with acromegaly. At the molecular level, reversal of GH-induced insulin resistance was accompanied by activation of insulin signalling in both skeletal muscle and adipose tissue mediated by downregulation of PTEN. Contrary to the classic metabolic syndrome, the improvement in insulin sensitivity occurred in concomitance with a reduction in lean body mass and an increase in fat mass.

GH acts on target tissues through the JAK/STAT signalling pathway that leads to phosphorylation and dimerization of STAT5, which in turn acts as transcription factor of target genes. The latter include SOCS/CISH, which feedback inhibits STAT5 phosphorylation[31] (Fig. 7). We have repeatedly observed STAT5 activation in human skeletal muscle and adipose tissue *in vivo* following exogenous GH exposure together with

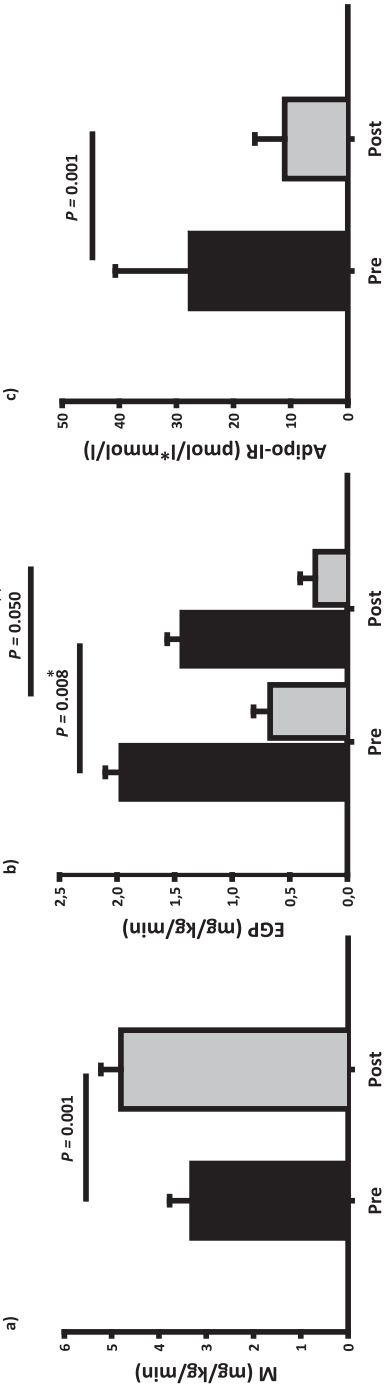

Fig. 3. Glucose metabolism and insulin sensitivity

Panel a: Mean ± SEM glucose infusion rate during the hyperinsulinemic euglycemic glucose clamp (HEC), expressed as M value, before (pre) and after (post) disease control. Panel b: Endogenous glucose production (EGP) in the basal state (black bars) and during the HEC (grey bars) before (pre) and after (post) disease control. Panel c: Mean ± SEM adipose tissue insulin resistance (Adipo-IR) before (pre) and after (post) disease control. Disease control increased insulin sensitivity in muscle (a), liver (b) and adipose tissue (c). *P** reflects the effect of disease control on EGP in the basal state and *P*** during the HEC.

increased mRNA expression of *CISH* and *SOCS*.[16,32-35] The present study is the first to document that sustained endogenous GH overproduction induces detectable activation of STAT5 signalling in adipose tissue, which illustrates the importance of adipose tissue as a direct GH target. We have previously reported that fatty acid infusion dampens GH-induced pSTAT5 expression in adipose tissue in healthy human subjects,[36] but the present data suggest that active acromegaly may override any such feedback suppression.

Acromegaly constitutes a unique combination of insulin resistance and a lean phenotype,[11,12,37] which was confirmed in the present study. Deterioration of glucose metabolism is observed in >50% of patients newly diagnosed with acromegaly[38] including glucose intolerance and overt diabetes mellitus.[38–40] Overall, glucose homeostasis improves after disease control in most[10,41,42] but not all studies.[43] We observed that disease control significantly improved peripheral and hepatic insulin sensitivity, regardless of treatment modality, which is in accordance with previous studies.[10,44] We also observed a reduced insulin—stimulated NOGD in active acromegaly suggesting impaired ability of insulin to stimulate glycogen synthesis as previously reported[44] or increased glucose cycling.[45] Resting energy expenditure was higher in patients with active acromegaly in accordance with previous studies.[10,46] This LBM-independent calorigenic effect of GH is not fully explained, but thyroid function is a recognized determinant of resting energy expenditure and we did observe slightly higher levels within the normal range of triiodothyronine in patients with active disease (data not shown) consistent with the known effect of GH on the peripheral conversion of T4 to T3.[47]

The GH-induced insulin resistance in muscle and liver is causally linked to lipolysis[4,48] but the underlying molecular mechanisms are not completely characterized. In the present study, active acromegaly was associated with a low fat mass, impaired insulin-stimulated anti-lipolysis and activation of the lipolytic pathway in adipose tissue, all of which are compatible with sustained GH-induced lipolysis (Fig. 7). Both endogenous and exogenous FFA suppress insulin-stimulated glucose uptake in skeletal muscle[49,50] and it is hypothesized that this process is mediated by competition between intermediates of glucose and fatty acids [5]. In support of this, we have previously observed that GH-induced insulin resistance is associated with suppressed pyruvate dehydrogenase activity.[6,51]

As an alternative mechanism of GH-induced insulin resistance in muscle, rodent and *in vitro* studies report GH-induced suppression of insulin signalling,[52–54] which until now has not been replicated in humans during short-term exposure to GH.[32,33,55] The present human study is therefore the first to observe GH-induced impairment of insulin signalling at the level of Akt activation, which constitutes a critical step in the

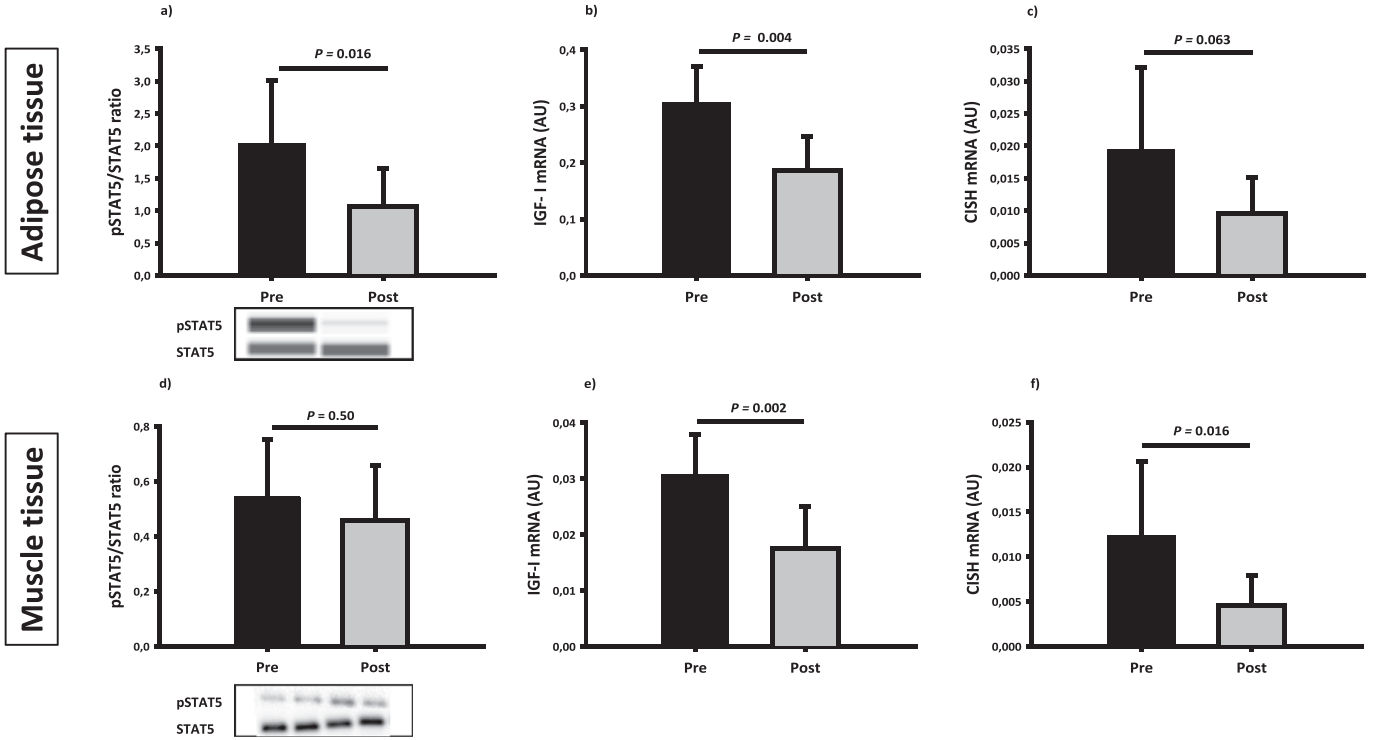

Fig. 4. GH signalling

Indices of GH signalling in adipose tissue and skeletal muscle tissue before (pre) and after (post) disease control. Upper panel: adipose tissue expression of total and phosphorylated STAT5 protein (a), *IGF-I* mRNA expression (b) and *CISH* mRNA (c). Lower panel: muscle tissue expression of total and phosphorylated STAT5 protein (d), mRNA expression of *IGF-I* (e) and *CISH* (f). P values reflect the effect of disease control in the basal state.

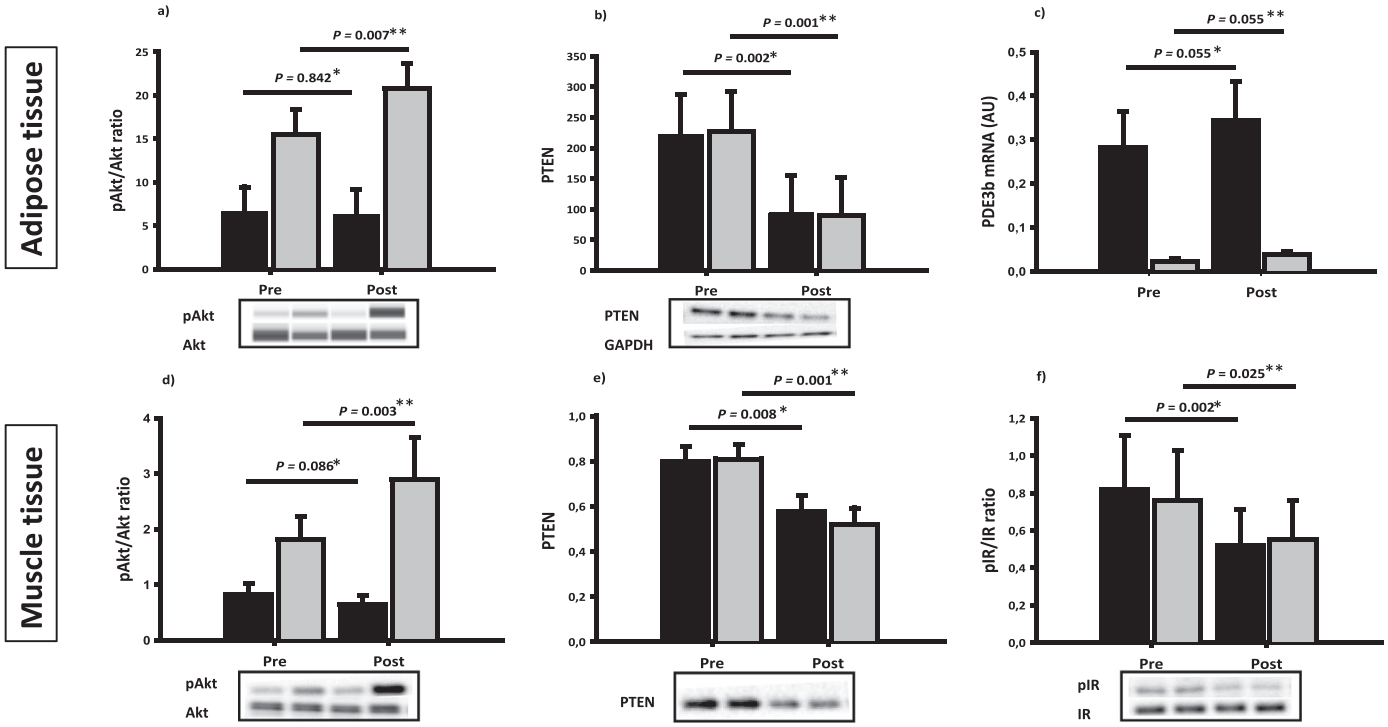

Fig. 5. Insulin signalling

Insulin signalling in adipose tissue and skeletal muscle in the basal state (black bars) and during the HEC (grey bars) before (pre) and after (post) disease control. Upper panel: adipose tissue expression of total and phosphorylated Akt protein (a), PTEN protein (b) and *PDE3b* mRNA (c). Lower panel: muscle tissue expression of total and phosphorylated Akt protein (d), PTEN protein (e) and total and phosphorylated IR protein (f). The effect of disease control on insulin signalling is presented in the basal state (*P**) and during the HEC (*P***).

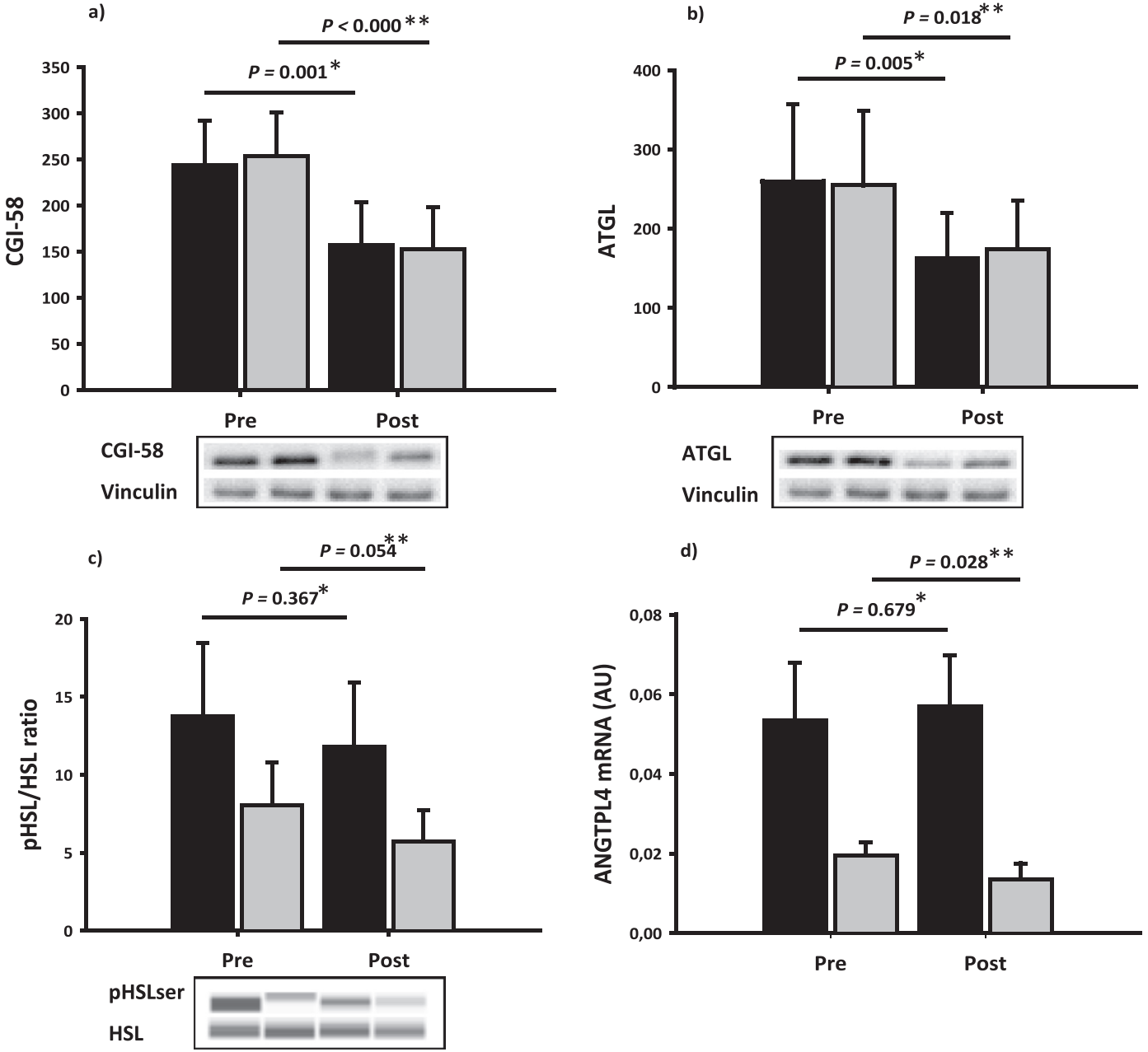

Fig. 6. Lipolysis

Lipolysis in adipose tissue in the basal state (black bars) and during the HEC (grey bars) before (pre) and after (post) disease control. Upper panel: adipose tissue expression of CGI-58 protein (a) and ATGL protein (b). Lower panel: adipose tissue expression of total and phosphorylated HSL protein (c) and *ANGTPL4* mRNA expression (d). The effect of disease control on lipolysis is presented in the basal state (*P**) and during the HEC (*P***).

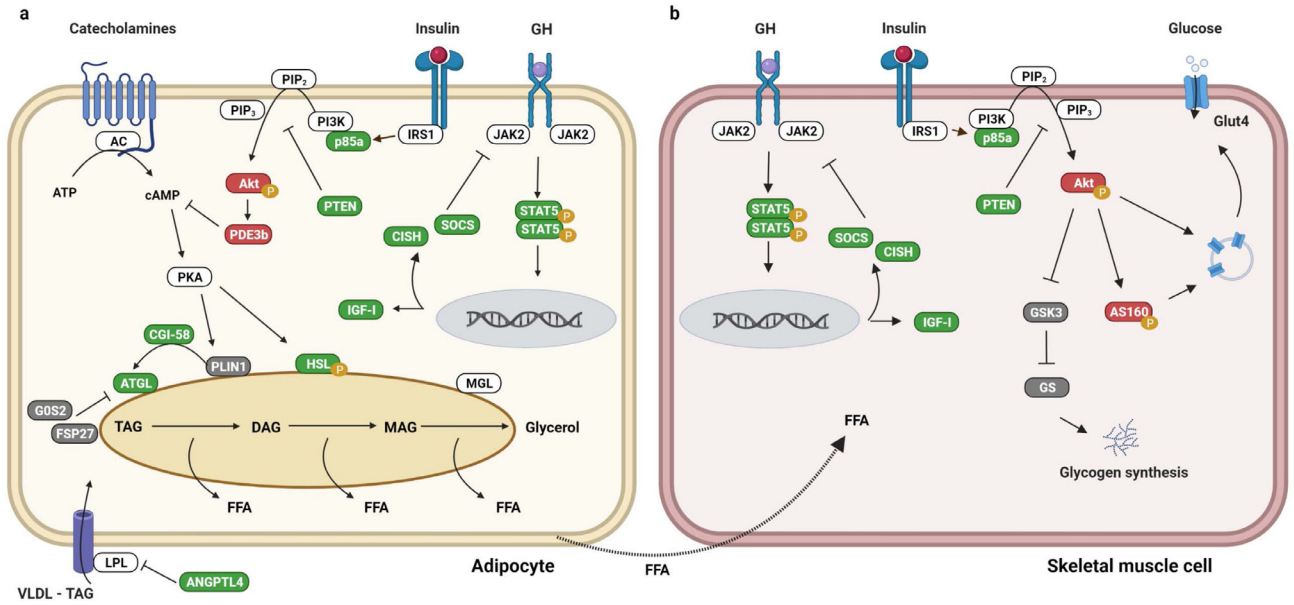

Fig. 7. Signalling pathways

Schematic presentation of signalling pathways in human adipocytes (left) and muscle cells (right) affected by GH and predominantly based on the present findings. Arrows indicate activation and truncated lines indicate inhibition. GH-induced upregulation/activation is shown in green and downregulation/inactivation in red. Unaltered regulation/activation is shown in grey.

'P' indicates phosphorylation. AC: adenyl cyclase, ATP: adenosenine triphosphate, DAG: diacylglycerol, MAG: monoacylglycerol, MGL: monoglyceride lipase, VLDL: very-low-density lipoproteins.

For further details, see the result and discussion sections of the manuscript.

pathway of insulin stimulated glucose uptake in skeletal muscle.[53] As a potential mediator, we concomitantly observed GH-induced upregulation of PTEN protein expression in both muscle and fat. PTEN is a negative regulator of PI3K signalling as it dephosphorylates phosphatidylinositol (3,4,5) bisphosphate (PIP_3) and thereby deactivates downstream signalling including Akt[56] (Fig. 7). In addition, the mRNA expression of *Pik3r1*, which encodes the regulatory p85α subunit of PI3K, was upregulated during prolonged GH excess. This is noteworthy since p85α protein excess may compete with the p85-p110 heterodimer for binding to insulin receptor substrate-1 (IRS-1),[8,57] which leads to inactivation of IRS-1-associated PI 3-kinase activity and ultimately inactivates Akt. Furthermore p85α has also been shown to upregulate PTEN.[58] Protein expression of PTEN and FFA concentrations correlated positively, supportive of a link between lipolysis and GH-induced suppression of insulin signalling. Evidence also suggests that SOCS proteins attenuates insulin signalling at the level of IR.[52,59,60] We also observed that *SOCS2* mRNA and PTEN protein correlated positively, which may support a suppressive effect of SOCS protein on insulin signalling. Surprisingly, we observed GH-induced activation of the IR, which most likely reflects increased IR binding and activation by IGF-I since cross-reactivity between insulin and IGF-I is well documented.[61,62] In support of this, we observed a strong positive correlation between IR activation and circulating IGF-I before disease control.

The impact of SA on glucose metabolism in acromegaly is ambiguous.[14,63-65] Somatostatin and its analogues directly suppress the pancreatic secretion of both insulin[21,66,67] and glucagon.[68] At the clinical level, meta-analyses report that SA treatment in acromegaly induces only a moderate impairment of glucose tolerance,[14,63] which may subside after long-term treatment.[69] We confirmed reduced glucose tolerance after SA, which was accompanied by a non-significant impairment of basal β-cell function (HOMA-β) and suppressed glucagon levels. By contrast, insulin sensitivity during the HEC improved markedly after SA treatment mediated by the concomitant suppression of GH secretion. However, mechanisms additional to GH suppression may contribute, since we have previously observed a peripheral stimulatory effect of somatostatin on insulin stimulated glucose uptake in human skeletal muscle.[17,18] We have also shown that SA treatment in patients with acromegaly activates Akt phosphorylation in response to an exogenous GH bolus.[16] In the present study, SA treatment also increased the forearm glucose uptake during the HEC together with increased protein expression of GLUT4 and αGSK. Taken together, this suggests that SA directly enhances peripheral glucose disposal by potentiating the actions of insulin in skeletal muscle.

Our data clearly demonstrated GH-induced insulin resistance in adipose tissue, which was accompanied by activation of both GH signalling and lipolytic signatures. Active acromegaly upregulated the protein expression of ATGL and HSL, both of which constitute rate-limiting steps of lipolysis. ATGL is activated by CGI-58,[70] which was upregulated in active acromegaly in our study. We have previously shown that short-term exogenous GH exposure downregulates G0S2 and FSP27, both of which are lipid droplet-associated suppressors of ATGL activity.[71–73] This was not observed in the present study, which may be explained by differences in the duration and degree of GH exposure. Active acromegaly also upregulated adipose tissue mRNA expression of *ANGPTL4*, which suppresses lipoprotein lipase (LPL) activity and thereby the uptake and storage of triacylglycerol (TAG) from the circulation.[74] We recently demonstrated that acute GH exposure also upregulates ANGPTL4 mRNA expression and suppresses LPL activity.[48] Taken together, it is plausible that active acromegaly is accompanied by reduced TAG uptake in addition to activated lipolysis in adipose tissue.

In addition to the direct regulatory effect of GH on lipolysis, and equivalent to the effects on skeletal muscle, GH dampened insulin signalling in adipose tissue. Akt is an insulin-dependent negative regulator of lipolysis, which via PD3b degrades cyclic adenosine monophosphate (cAMP) and thereby inactivates protein kinase A (PKA) (72). Protein kinase A, in turn, reduces the phosphorylation of HSL and perilipin 1 (PLIN1),[75] In the present study, we observed a GH-induced downregulation of Akt activation as well as down regulation of *PDE3b* mRNA expression (Fig. 7). In addition to our findings in skeletal muscle, we observed GH-induced upregulation of PTEN in adipose tissue where it acts to suppress insulin-induced anti-lipolysis.[75] Studies in rodents report that tissue-specific PTEN loss in muscle, liver and adipose tissue increases insulin sensitivity,[76–78] and studies in humans have reported a GH-induced upregulation of PTEN mRNA expression in adipose tissue.[71,72,79] Taken together, this suggests that reversible suppression of insulin signalling in both muscle and fat is a distinct feature of active acromegaly with upregulation of PTEN as a putative pivotal node (Fig. 7).

Certain limitations of this study merit attention. First, only a limited number of biopsies were drawn during the studies, which reduces the temporal resolution and inherent limitations apply to protein blotting and PCR techniques. Second, the sample size was relatively small, which imposes the risk of type 2 errors. The heterogeneity of the treatment patterns of our study may impact our results but it reflects real life data. Finally, the design of the study does not provide information about the mechanistic interaction between GH and insulin signalling, which remains to be further characterized.

In summary, this study provides a unique *in vivo* demonstration of insulin resistance unrelated to the

metabolic syndrome in which primary activation of lipolysis seems the most plausible mechanism. At the molecular level, suppressed insulin signalling underpinned insulin resistance in both muscle and adipose tissue paralleled by reversible activation of canonical GH signalling pathways, and we suggest that GH-induced upregulation PTEN constitutes a pivotal node in this context.

Contributors

MCAS and JOLJ had full access to all the data in the study and takes responsibility for the integrity of the data and the accuracy of the data analysis. MCAS, NJ and JOLJ designed the study. MCAS, JD, MAM, MLH, AJH, SBP and NM acquired the data and carried out the data analysis. MCAS and JOLJ drafted the manuscript. All authors made substantial contributions to the interpretation of the results and critical revision of the manuscript. All authors approved the final version of the manuscript.

Declaration of Competing Interest

JOLJ and JD have received unrestricted research grants and lecture fees from Pfizer and IPSEN.

Acknowledgements

The authors thank Helle Zibrandtsen and Lenette Pedersen for excellent technical assistance during the study. This work was supported in part a by grant from the Independent Research Fund, Denmark (7016-00303A) and from the Alfred Benzon Foundation, Denmark.

Data sharing section

The dataset generated and analysed during the current study is available from the corresponding author on request.

Supplementary materials

Supplementary material associated with this article can be found in the online version at doi: 10.1016/j.ebiom.2021.103763.

References

1 Dal J, Feldt-Rasmussen U, Andersen M, et al. Acromegaly incidence, prevalence, complications and long-term prognosis: a nationwide cohort study. *Eur J Endocrinol* 2016;**175**(3):181–90.
2 Moller N, Jorgensen JO. Effects of growth hormone on glucose, lipid, and protein metabolism in human subjects. *Endocr Rev* 2009;**30**(2):152–77.
3 Katznelson L, Laws Jr. ER, Melmed S, et al. Acromegaly: an endocrine society clinical practice guideline. *J Clin Endocrinol Metab* 2014;**99**(11):3933–51.
4 Nielsen S, Moller N, Christiansen JS, Jorgensen JO. Pharmacological antilipolysis restores insulin sensitivity during growth hormone exposure. *Diabetes* 2001;**50**(10):2301–8.
5 Randle PJ, Garland PB, Hales CN, Newsholme EA. The glucose fatty-acid cycle. Its role in insulin sensitivity and the metabolic disturbances of diabetes mellitus. *Lancet* 1963;**1**(7285):785–9.
6 Nellemann B, Vendelbo MH, Nielsen TS, et al. Growth hormone-induced insulin resistance in human subjects involves reduced pyruvate dehydrogenase activity. *Acta Physiol (Oxf)* 2014;**210**(2):392–402.
7 Bak JF, Moller N, Schmitz O. Effects of growth hormone on fuel utilization and muscle glycogen synthase activity in normal humans. *Am J Physiol* 1991;**260**(5 Pt 1):E736–42.
8 del Rincon JP, Iida K, Gaylinn BD, et al. Growth hormone regulation of p85alpha expression and phosphoinositide 3-kinase activity in adipose tissue: mechanism for growth hormone-mediated insulin resistance. *Diabetes* 2007;**56**(6):1638–46.
9 Pan XR, Li GW, Hu YH, et al. Effects of diet and exercise in preventing NIDDM in people with impaired glucose tolerance. The Da Qing IGT and Diabetes Study. *Diabetes Care* 1997;**20**(4):537–44.
10 Moller N, Schmitz O, Joorgensen JO, et al. Basal- and insulin-stimulated substrate metabolism in patients with active acromegaly before and after adenomectomy. *J Clin Endocrinol Metab* 1992;**74**(5):1012–9.
11 Reyes-Vidal CM, Mojahed H, Shen W, et al. Adipose Tissue Redistribution and Ectopic Lipid Deposition in Active Acromegaly and Effects of Surgical Treatment. *J Clin Endocrinol Metab* 2015;**100**(8):2946–55.
12 Freda PU, Shen W, Heymsfield SB, et al. Lower visceral and subcutaneous but higher intermuscular adipose tissue depots in patients with growth hormone and insulin-like growth factor I excess due to acromegaly. *J Clin Endocrinol Metab* 2008;**93**(6):2334–43.
13 Melmed S, Casanueva F, Cavagnini F, et al. Consensus statement: medical management of acromegaly. *Eur J Endocrinol* 2005;**153**(6):737–40.
14 Mazziotti G, Floriani I, Bonadonna S, Torri V, Chanson P, Giustina A. Effects of somatostatin analogs on glucose homeostasis: a meta-analysis of acromegaly studies. *J Clin Endocrinol Metab* 2009;**94**(5):1500–8.
15 Alberti KG, Christensen NJ, Christensen SE, et al. Inhibition of insulin secretion by somatostatin. *Lancet* 1973;**2**(7841):1299–301.
16 Dal J, Hoyer KL, Pedersen SB, et al. Growth Hormone and Insulin Signaling in Acromegaly: Impact of Surgery Versus Somatostatin Analog Treatment. *J Clin Endocrinol Metab* 2016;**101**(10):3716–23.
17 Krusenstjerna-Hafstrom T, Vestergaard ET, Buhl M, et al. Acute peripheral metabolic effects of intraarterial leg infusion of somatostatin in healthy young men. *J Clin Endocrinol Metab* 2011;**96**(8):2581–9.
18 Moller N, Bagger JP, Schmitz O, et al. Somatostatin enhances insulin-stimulated glucose uptake in the perfused human forearm. *J Clin Endocrinol Metab* 1995;**80**(6):1789–93.
19 Neggers SJ, Franck SE, de Rooij FW, et al. Long-term efficacy and safety of pegvisomant in combination with long-acting somatostatin analogs in acromegaly. *J Clin Endocrinol Metab* 2014;**99**(10):3644–52.
20 Kopchick JJ, Parkinson C, Stevens EC, Trainer PJ. Growth hormone receptor antagonists: discovery, development, and use in patients with acromegaly. *Endocr Rev* 2002;**23**(5):623–46.
21 Strowski MZ, Parmar RM, Blake AD, Schaeffer JM. Somatostatin inhibits insulin and glucagon secretion via two receptors subtypes: an in vitro study of pancreatic islets from somatostatin receptor 2 knockout mice. *Endocrinology* 2000;**141**(1):111–7.
22 Bidlingmaier M, Friedrich N, Emeny RT, et al. Reference intervals for insulin-like growth factor-1 (igf-i) from birth to senescence: results from a multicenter study using a new automated chemiluminescence IGF-I immunoassay conforming to recent international recommendations. *J Clin Endocrinol Metab* 2014;**99**(5):1712–21.
23 Wallace TM, Levy JC, Matthews DR. Use and abuse of HOMA modeling. *Diabetes Care* 2004;**27**(6):1487–95.
24 Sondergaard E, Espinosa De Ycaza AE, Morgan-Bathke M, Jensen MD. How to Measure Adipose Tissue Insulin Sensitivity. *J Clin Endocrinol Metab* 2017;**102**(4):1193–9.
25 Cooper KE, Edholm OG, Mottram RF. The blood flow in skin and muscle of the human forearm. *J Physiol* 1955;**128**(2):258–67.
26 Muller MJ, Illner K, Bosy-Westphal A, Brinkmann G, Heller M. Regional lean body mass and resting energy expenditure in non-obese adults. *Eur J Nutr* 2001;**40**(3):93–7.
27 Ferrannini E. The theoretical bases of indirect calorimetry: a review. *Metabolism* 1988;**37**(3):287–301.
28 Vigelso A, Dybboe R, Hansen CN, Dela F, Helge JW, Guadalupe Grau A. GAPDH and beta-actin protein decreases with aging, making Stain-Free technology a superior loading control in Western blotting of human skeletal muscle. *J Appl Physiol (1985)* 2015;**118**(3):386–94.

29 Lu J, Allred CC, Jensen MD. Human adipose tissue protein analyses using capillary western blot technology. *Nutr Diabetes* 2018;**8**(1):26.
30 Okorodudu DO, Jumean MF, Montori VM, et al. Diagnostic performance of body mass index to identify obesity as defined by body adiposity: a systematic review and meta-analysis. *Int J Obes (Lond)* 2010;**34**(5):791–9.
31 Schindler C, Levy DE, Decker T. JAK-STAT signaling: from interferons to cytokines. *J Biol Chem* 2007;**282**(28):20059–63.
32 Nielsen C, Gormsen LC, Jessen N, et al. Growth hormone signaling in vivo in human muscle and adipose tissue: impact of insulin, substrate background, and growth hormone receptor blockade. *J Clin Endocrinol Metab* 2008;**93**(7):2842–50.
33 Jorgensen JO, Jessen N, Pedersen SB, et al. GH receptor signaling in skeletal muscle and adipose tissue in human subjects following exposure to an intravenous GH bolus. *Am J Physiol Endocrinol Metab* 2006;**291**(5):E899–905.
34 Hogild ML, Bak AM, Pedersen SB, et al. Growth hormone signaling and action in obese versus lean human subjects. *Am J Physiol Endocrinol Metab* 2019;**316**(2):E333–44.
35 Moller L, Dalman L, Norrelund H, et al. Impact of fasting on growth hormone signaling and action in muscle and fat. *J Clin Endocrinol Metab* 2009;**94**(3):965–72.
36 Moller N, Gormsen LC, Schmitz O, Lund S, Jorgensen JO, Jessen N. Free fatty acids inhibit growth hormone/signal transducer and activator of transcription-5 signaling in human muscle: a potential feedback mechanism. *J Clin Endocrinol Metab* 2009;**94**(6):2204–7.
37 Bengtsson BA, Brummer RJ, Bosaeus I. Growth hormone and body composition. *Horm Res* 1990;**33**(Suppl 4):19–24.
38 Alexopoulou O, Bex M, Kamenicky P, Mvoula AB, Chanson P, Maiter D. Prevalence and risk factors of impaired glucose tolerance and diabetes mellitus at diagnosis of acromegaly: a study in 148 patients. *Pituitary* 2014;**17**(1):81–9.
39 Colao A, Ferone D, Marzullo P, Lombardi G. Systemic complications of acromegaly: epidemiology, pathogenesis, and management. *Endocr Rev* 2004;**25**(1):102–52.
40 Fieffe S, Morange I, Petrossians P, et al. Diabetes in acromegaly, prevalence, risk factors, and evolution: data from the French Acromegaly Registry. *Eur J Endocrinol* 2011;**164**(6):877–84.
41 Kinoshita Y, Fujii H, Takeshita A, et al. Impaired glucose metabolism in Japanese patients with acromegaly is restored after successful pituitary surgery if pancreatic {beta}-cell function is preserved. *Eur J Endocrinol* 2011;**164**(4):467–73.
42 He W, Yan L, Wang M, et al. Surgical outcomes and predictors of glucose metabolism alterations for growth hormone-secreting pituitary adenomas: a hospital-based study of 151 cases. *Endocrine* 2019;**63**(1):27–35.
43 Jonas C, Maiter D, Alexopoulou O. Evolution of Glucose Tolerance After Treatment of Acromegaly: A Study in 57 Patients. *Horm Metab Res* 2016;**48**(5):299–305.
44 Foss MC, Saad MJ, Paccola GM, Paula FJ, Piccinato CE, Moreira AC. Peripheral glucose metabolism in acromegaly. *J Clin Endocrinol Metab* 1991;**72**(5):1048–53.
45 Karlander S, Vranic M, Efendic S. Increased glucose turnover and glucose cycling in acromegalic patients with normal glucose tolerance. *Diabetologia* 1986;**29**(11):778–83.
46 O'Sullivan AJ, Kelly JJ, Hoffman DM, Baxter RC, Ho KK. Energy metabolism and substrate oxidation in acromegaly. *J Clin Endocrinol Metab* 1995;**80**(2):486–91.
47 Jorgensen JO, Moller J, Laursen T, Orskov H, Christiansen JS, Weeke J. Growth hormone administration stimulates energy expenditure and extrathyroidal conversion of thyroxine to triiodothyronine in a dose-dependent manner and suppresses circadian thyrotrophin levels: studies in GH-deficient adults. *Clin Endocrinol (Oxf)* 1994;**41**(5):609–14.
48 Hjelholt AJ, Sondergaard E, Pedersen SB, Moller N, Jessen N, Jorgensen JOL. Growth hormone upregulates ANGPTL4 mRNA and suppresses lipoprotein lipase via fatty acids: Randomized experiments in human individuals. *Metabolism* 2020;**105**:154188.
49 Zierler KL, Rabinowitz D. Roles of Insulin and Growth Hormone, Based on Studies of Forearm Metabolism in Man. *Medicine (Baltimore)* 1963;**42**:385–402.
50 Roden M, Price TB, Perseghin G, et al. Mechanism of free fatty acid-induced insulin resistance in humans. *J Clin Invest* 1996;**97**(12):2859–65.
51 Hjelholt AJ, Charidemou E, Griffin JL, et al. Insulin resistance induced by growth hormone is linked to lipolysis and associated with suppressed pyruvate dehydrogenase activity in skeletal muscle: a 2 x 2 factorial, randomised, crossover study in human individuals. *Diabetologia* 2020.
52 Ueki K, Kondo T, Kahn CR. Suppressor of cytokine signaling 1 (SOCS-1) and SOCS-3 cause insulin resistance through inhibition of tyrosine phosphorylation of insulin receptor substrate proteins by discrete mechanisms. *Mol Cell Biol* 2004;**24**(12):5434–46.
53 Taniguchi CM, Emanuelli B, Kahn CR. Critical nodes in signalling pathways: insights into insulin action. *Nat Rev Mol Cell Biol* 2006;**7**(2):85–96.
54 Dominici FP, Argentino DP, Munoz MC, Miquet JG, Sotelo AI, Turyn D. Influence of the crosstalk between growth hormone and insulin signalling on the modulation of insulin sensitivity. *Growth Horm IGF Res* 2005;**15**(5):324–36.
55 Jessen N, Djurhuus CB, Jorgensen JO, et al. Evidence against a role for insulin-signaling proteins PI 3-kinase and Akt in insulin resistance in human skeletal muscle induced by short-term GH infusion. *Am J Physiol Endocrinol Metab* 2005;**288**(1):E194–9.
56 Carracedo A, Pandolfi PP. The PTEN-PI3K pathway: of feedbacks and cross-talks. *Oncogene* 2008;**27**(41):5527–41.
57 Barbour LA, Mizanoor Rahman S, Gurevich I, et al. Increased P85alpha is a potent negative regulator of skeletal muscle insulin signaling and induces in vivo insulin resistance associated with growth hormone excess. *J Biol Chem* 2005;**280**(45):37489–94.
58 Taniguchi CM, Tran TT, Kondo T, et al. Phosphoinositide 3-kinase regulatory subunit p85alpha suppresses insulin action via positive regulation of PTEN. *Proc Natl Acad Sci U S A* 2006;**103**(32):12093–7.
59 Rui L, Yuan M, Frantz D, Shoelson S, White MF. SOCS-1 and SOCS-3 block insulin signaling by ubiquitin-mediated degradation of IRS1 and IRS2. *J Biol Chem* 2002;**277**(44):42394–8.
60 Emanuelli B, Peraldi P, Filloux C, et al. SOCS-3 inhibits insulin signaling and is up-regulated in response to tumor necrosis factor-alpha in the adipose tissue of obese mice. *J Biol Chem* 2001;**276**(51):47944–9.
61 Belfiore A, Frasca F, Pandini G, Sciacca L, Vigneri R. Insulin receptor isoforms and insulin receptor/insulin-like growth factor receptor hybrids in physiology and disease. *Endocr Rev* 2009;**30**(6):586–623.
62 Hakuno F, Takahashi SI. IGF1 receptor signaling pathways. *J Mol Endocrinol* 2018;**61**(1):T69–86.
63 Cozzolino A, Feola T, Simonelli I, et al. Somatostatin Analogs and Glucose Metabolism in Acromegaly: A Meta-analysis of Prospective Interventional Studies. *J Clin Endocrinol Metab* 2018.
64 Ho KK, Jenkins AB, Furler SM, Borkman M, Chisholm DJ. Impact of octreotide, a long-acting somatostatin analogue, on glucose tolerance and insulin sensitivity in acromegaly. *Clin Endocrinol (Oxf)* 1992;**36**(3):271–9.
65 Baldelli R, Battista C, Leonetti F, et al. Glucose homeostasis in acromegaly: effects of long-acting somatostatin analogues treatment. *Clin Endocrinol (Oxf)* 2003;**59**(4):492–9.
66 Giustina A, Mazziotti G, Maffezzoni F, Amoroso V, Berruti A. Investigational drugs targeting somatostatin receptors for treatment of acromegaly and neuroendocrine tumors. *Expert Opin Investig Drugs* 2014;**23**(12):1619–35.
67 Singh V, Brendel MD, Zacharias S, et al. Characterization of somatostatin receptor subtype-specific regulation of insulin and glucagon secretion: an in vitro study on isolated human pancreatic islets. *J Clin Endocrinol Metab* 2007;**92**(2):673–80.
68 Davies RR, Miller M, Turner SJ, et al. Effects of somatostatin analogue SMS 201-995 in normal man. *Clin Endocrinol (Oxf)* 1986;**24**(6):665–74.
69 Colao A, Auriemma RS, Galdiero M, et al. Impact of somatostatin analogs versus surgery on glucose metabolism in acromegaly: results of a 5-year observational, open, prospective study. *J Clin Endocrinol Metab* 2009;**94**(2):528–37.
70 Granneman JG, Moore HP, Granneman RL, Greenberg AS, Obin MS, Zhu Z. Analysis of lipolytic protein trafficking and interactions in adipocytes. *J Biol Chem* 2007;**282**(8):5726–35.
71 Hjelholt AJ, Lee KY, Arlien-Soborg MC, et al. Temporal patterns of lipolytic regulators in adipose tissue after acute growth hormone exposure in human subjects: A randomized controlled crossover trial. *Mol Metab* 2019;**29**:65–75.
72 Hoyer KL, Hogild ML, List EO, et al. The acute effects of growth hormone in adipose tissue is associated with suppression of antilipolytic signals. *Physiol Rep* 2020;**8**(3):e14373.
73 Sharma VM, Vestergaard ET, Jessen N, et al. Growth hormone acts along the PPARgamma-FSP27 axis to stimulate lipolysis in human adipocytes. *Am J Physiol Endocrinol Metab* 2019;**316**(1):E34–42.

74 Richelsen B. Action of growth hormone in adipose tissue. *Horm Res* 1997;**48**(Suppl 5):105–10.

75 Nielsen TS, Jessen N, Jorgensen JO, Moller N, Lund S. Dissecting adipose tissue lipolysis: molecular regulation and implications for metabolic disease. *J Mol Endocrinol* 2014;**52**(3):R199–222.

76 Stiles B, Wang Y, Stahl A, et al. Liver-specific deletion of negative regulator Pten results in fatty liver and insulin hypersensitivity [corrected]. *Proc Natl Acad Sci U S A* 2004;**101**(7):2082–7.

77 Kurlawalla-Martinez C, Stiles B, Wang Y, Devaskar SU, Kahn BB, Wu H. Insulin hypersensitivity and resistance to streptozotocin-induced diabetes in mice lacking PTEN in adipose tissue. *Mol Cell Biol* 2005;**25**(6):2498–510.

78 Wijesekara N, Konrad D, Eweida M, et al. Muscle-specific Pten deletion protects against insulin resistance and diabetes. *Mol Cell Biol* 2005;**25**(3):1135–45.

79 Pedersen MH, Svart MV, Lebeck J, et al. Substrate Metabolism and Insulin Sensitivity During Fasting in Obese Human Subjects: Impact of GH Blockade. *J Clin Endocrinol Metab* 2017;**102**(4):1340–9.